



ELSEVIER

Available online at www.sciencedirect.com

 ScienceDirect

International Journal of Solids and Structures 43 (2006) 7407–7423

INTERNATIONAL JOURNAL OF
**SOLIDS and
STRUCTURES**

www.elsevier.com/locate/ijsolstr

Instability leading to coal bumps and nonlinear evolutionary mechanisms for a coal-pillar-and-roof system

Siqing Qin ^{a,*}, Jiu Jimmy Jiao ^b, C.A. Tang ^c, Zhigang Li ^a

^a *Engineering Geology and Applied Geophysics Department, Institute of Geology and Geophysics, Chinese Academy of Sciences, P.O. Box 9825, Beijing 100029, People's Republic of China*

^b *Department of Earth Sciences, The University of Hong Kong, Pokfulam Road, Hong Kong, People's Republic of China*

^c *Centre for Rockbursts and Induced Seismicity Research, Northeastern University, Shenyang, People's Republic of China*

Received 17 January 2005; received in revised form 31 May 2005

Available online 27 September 2006

Abstract

This paper studies the unstable mechanisms of the mechanical system that is composed of the stiff hosts (roof and floor) and the coal pillar using catastrophe theory. It is assumed that the roof is an elastic beam and the coal pillar is a strain-softening medium which can be described by the Weibull's distribution theory of strength. It is found that the instability leading to coal bump depends mainly on the system's stiffness ratio k , which is defined as the ratio of the flexural stiffness of the beam to the absolute value of the stiffness at the turning point of the constitutive curve of the coal pillar, and the homogeneity index m or shape parameter of the Weibull's distribution for the coal pillar. The applicability of the cusp catastrophe is demonstrated by applying the equations to the Mentougou coal mine. A nonlinear dynamical model, which is derived by considering the time-dependent property of the coal pillar, is used to study the physical prediction of coal bumps. An algorithm of inversion for determining the parameters of the nonlinear dynamical model is suggested for seeking the precursory abnormality from the observed series of roof settlement. A case study of the Muchengjian coal mine is conducted and its nonlinear dynamical model is established from the observation series using the algorithm of inversion. An important finding is that the catastrophic characteristic index D (i.e., the bifurcation set of the cusp catastrophe model) drastically increases to a high peak value and then quickly drops close to instability. From the viewpoint of damage mechanics of coal pillar, a dynamical model of acoustic emission (AE) is established for modeling the AE activities in the evolutionary process of the system. It is revealed that the values of m and the evolutionary path ($D = 0$ or $D \neq 0$) of the system have a great impact on the AE activity patterns and characters. © 2006 Elsevier Ltd. All rights reserved.

Keywords: Cusp catastrophe; Instability; Stiffness ratio; Nonlinear; Physical prediction; Acoustic emission

* Corresponding author. Fax: +86 10 620 405 74.

E-mail address: qinsiqing@hotmail.com (S. Qin).

1. Introduction

Rockbursts and bumps are experienced in underground mining at various locations in the world, causing death and serious injury to underground miners and damage to mine facilities (Chen et al., 1997). Although the phenomenon of rockburst or bump had been experienced in mines since the 18th century, a better understanding of rockburst or bump was initially made through the experimental work of Cook (1965), which provides the first theoretical analysis of rockburst or bump developed from experimental results. Since the 1950s, significant achievements have been made in systematic studies on the dynamical behavior of mining-induced rockbursts and bumps upon the knowledge of rock mechanics (Salamon, 1993; Kaiser et al., 1995). Many theoretical and numerical models and technical means have been developed in mechanism analysis and prevention of rockburst or bump (Tang et al., 1993; Wang and Park, 2001). However, in the field of mining and geomechanics, there are great challenges to better understand, predict, control the condition of rockburst or bump during underground mining and construction.

Some preventive and monitoring approaches (Xie and Pariseau, 1993), such as the affusion method, micro-gravity method, rheological method, rebound method, drilling-yield method, and micro-seismics method, have been applied in many underground openings for understanding the mechanisms of rockbursts and bumps and predicting their occurrence. However, few approaches have been found to be particularly successful. The reason for this may be due to (1) that the precise physical mechanisms of rockbursts is very complicated and, therefore, it is difficult to establish a simple mechanical model for rockbursts or bumps; and (2) the seismic data monitored in situ are not completely or appropriately utilized (Chen et al., 1997).

In underground openings, seismic activity or acoustic emission (AE) is often a concern because related dynamical effects may lead to violent failure and support damage (Kaiser and Tang, 1998). Furthermore, seismicity has become an important indicator for assessing the stability of rock excavations, particularly in mining engineering. As pointed out by Kaiser (1995), “now that most deep mines have installed micro-seismic monitoring systems, the challenge is to find means to integrate AE or micro-seismic source location and source parameter data into the model calibration process”. Consequently, it is necessary to analyze the seismic behavior of rock by analytical or numerical methods.

The previous research on judging the occurrence of rockbursts and bumps is based mainly on the conventional strength criterion. However, the rock or coal failures may occur in a progressive manner, which may not always lead to rockbursts and bumps. Thus, the strength criterion may be inappropriate for judging the occurrence of rockburst or bump. It is well known from tests with a stiff, servo-controlled testing machine (Hudson et al., 1972) that the failure process, the related AE or seismicity, and the degree of instability depend on the stiffness of the loading system. The mining geometry and the properties of the rock mass in the pillar and the surrounding rock control the system stiffness and, thus, the behavior of the pillar.

The methods and approaches based on the catastrophe theory developed by Thom (1972) have been recently applied to investigate various problems in geology and geomechanics (Henley, 1976; Pan and Zhang, 1992; Qin et al., 1993; Tang, 1993; Tang et al., 1993; Xu et al., 1995; Qin et al., 2001). A brief review of these applications can be found in the paper by Qin et al., 2001. Most rockbursts and bumps can be regarded as a discontinuous catastrophe phenomenon. Thus, it is appropriate to study rockbursts and bumps using the catastrophe theory. Pan and Zhang (1992) presented a cusp catastrophe model by regarding the roof and the coal pillar as a testing machine and coal specimen system. Qin et al. (1993) and Xu et al. (1995) studied the unstable mechanisms of the coal-pillar-and-roof system by the catastrophe theory. They described the stress–strain constitutive model of the coal pillar by a negative exponent distribution of strength, but did not deal with the dynamical process and AE mechanisms in the deformation of the coal-pillar-and-roof system, which are key issues to be investigated in this paper.

This paper is a generalization and extension of the previous studies. The stress–strain constitutive model for the coal pillar is described by the Weibull’s distribution law, which is more general and practical than a negative exponent distribution. A cusp catastrophe model will be presented for the system that is composed

of the coal pillar and stiff host rock (roof and floor). The unstable conditions of such a system leading to coal bump will be suggested using the catastrophe theory. Furthermore, by considering the time-dependent and damaged properties of the coal pillar, a nonlinear dynamical model and an AE dynamical model will also be put forward for studying the physical prediction of coal bump and AE characteristics in the deformation process of the system.

2. Cusp catastrophe model and instability mechanisms

2.1. Mechanical model

Some of the coal bumps in underground openings occur in multifarious coal pillars. The coal pillars are usually pre-preserved for supporting the roof under the condition of both hard rock roof and hard rock floor when the pillar-and-room method or the pillar-and-board method is applied for coal mining. While the progressive failures result in coal bumps in the coal pillars, such as Datong and Sanhejian coal mines in China, the rock layers of the roof are unbroken and are concerned only with energy release. Considering that the excavation width l at the underground coal chamber is fairly great and approximately symmetrical, and that the coal pillar width b and the roof thickness h_b are far smaller than the excavation width l , we can hence regard the rock layer of the roof as an elastic beam (Fig. 1). The self-weight of the beam and the weight of the upper strata are simplified as the distribution force with the gravitational load intensity q acting above the beam top. Under the above assumptions, the compression deformation of the coal pillar will be much larger than that of the unmined coal bed. For simplicity, it is assumed that the unmined coal bed is

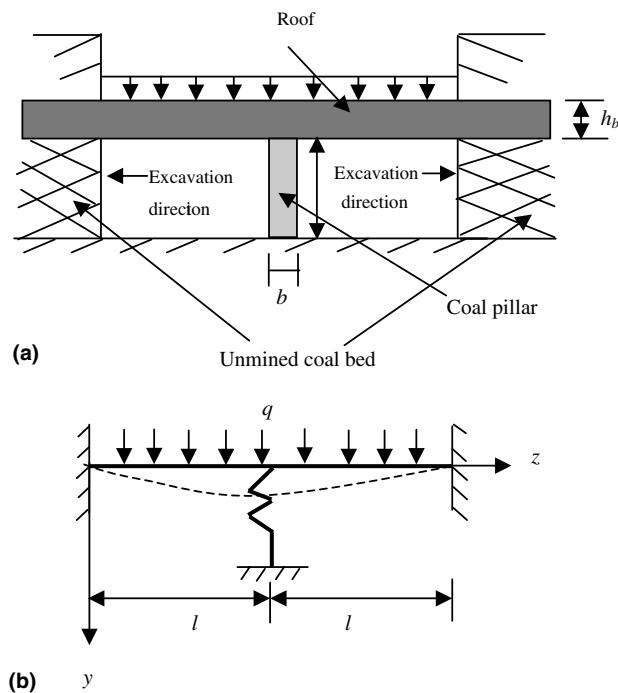


Fig. 1. Mechanical model of coal-pillar-and-roof system using pillar-and-room method for coal mining; (a) Sketch map of pillar-and-room method for coal mining; (b) interacting mechanical model for the coal-pillar-and-roof system.

stiff and the beam is built-in. The mechanical model for the coal-pillar-and-beam system is illustrated in Fig. 1.

According to damage mechanics (Krajcinovic and Silva, 1982), the constitutive laws of rock or coal under uniaxial stress conditions can be expressed as

$$\sigma = E\varepsilon[1 - D(\varepsilon)] \quad (1)$$

where σ , ε and E are the stress, the strain and the elastic modulus of the rock or coal specimen, respectively; $D(\varepsilon)$ is termed the damage parameter.

The constitutive model of the coal pillar is a nonlinear one with the strain-softening property. Pan and Zhang (1992), Qin et al. (1993), and Xu et al. (1995) once used a negative exponent distribution of strength to describe the strain-softening property. However, the most commonly used distribution is Weibull's distribution which describes very well the experimental data (Hudson and Fairhurst, 1969; Tang, 1993; Qin et al., 1999). Here we adopt the Weibull's distribution law for the strain-softening media. That is

$$\sigma = E\varepsilon \exp \left[-\left(\frac{\varepsilon}{\varepsilon_0}\right)^m \right] \quad (2)$$

$$D(\varepsilon) = 1 - \exp \left[-\left(\frac{\varepsilon}{\varepsilon_0}\right)^m \right] \quad (3)$$

where ε_0 is a measurement of average strain and m is the shape parameter. One of the attractive aspects of the Weibull's distribution is the presence of the shape parameter which allows this function to take a wide variety of shapes (Fig. 2). For instance, for $m = 1$, this distribution is exponential; at about $m = 2$, it very closely approximates a normal distribution. Since m is a measurement of the local strength variability, it can be considered as a homogeneity index (Tang, 1993). The larger the index m , the more homogeneous is the rock. When m trends to infinity, the variance trends to zero and a fully homogeneous rock is obtained. A material with such a property is so-called ideal brittle material, such as glass. Thus, the shape parameter m can also be referred to as the brittleness index.

For the coal pillar with a sectional area A and a height h , Eq. (2) can also be expressed as the following equation in terms of the load P and deformation u :

$$P = k_0 u \exp \left[-\left(\frac{u}{u_0}\right)^m \right] \quad (4)$$

where $k_0 = \frac{EA}{h}$ is the initial stiffness of the coal pillar. It is easily verified that the displacement value at the turning point of $P-u$ curve is equal to $u_0 \left(\frac{m+1}{m}\right)^{1/m}$ by $\frac{d^2P}{du^2} = 0$. According to the material mechanics theory (Liu, 1991), the moment equilibrium equation of the beam is

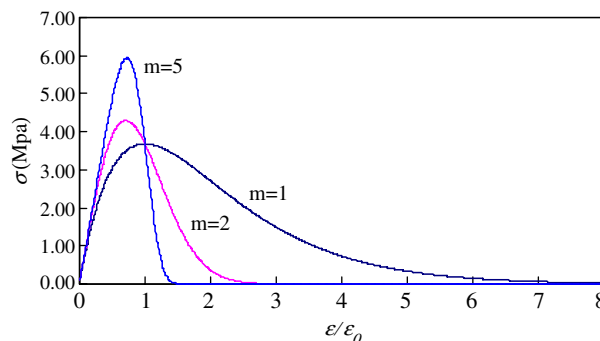


Fig. 2. Weibull's distribution constitutive curves for different values of m ($E = 100$ MPa and $\varepsilon_0 = 0.1$).

$$E_e I y'' = \frac{1}{2} q z^2 - \left(q l - \frac{1}{2} P \right) z + \frac{1}{3} q l^2 - \frac{1}{4} P l \tag{5}$$

where E_e and I are the Young’s modulus and the moment of inertia of the beam, respectively. Integrating Eq. (5) twice and using the known boundary condition $y'(0) = y(0) = 0$, one has

$$E_e I y = \frac{1}{24} q z^4 - \frac{1}{6} \left(q l - \frac{1}{2} P \right) z^3 + \frac{1}{2} \left(\frac{1}{3} q l^2 - \frac{1}{4} P l \right) z^2 \tag{6}$$

Using the deformation continuum condition of the deflection value u at $z = l$ and substituting Eq. (4) into (6), one obtains

$$P = k_0 u \exp \left[- \left(\frac{u}{u_0} \right)^m \right] = q l - \frac{24 E_e I}{l^3} u \tag{7}$$

2.2. Cusp catastrophe model

For the mechanical system that is composed of the beam and coal pillar, as illustrated in Fig. 1, the equilibrium condition of forces (or called the equilibrium surface in Fig. 3) can be derived as follows

$$\frac{dV}{du} = k_0 u \exp \left[- \left(\frac{u}{u_0} \right)^m \right] + \frac{24 E_e I}{l^3} u - q l = 0 \tag{8}$$

where V is the potential energy of the system.

The cusp can be solved by the smoothness property of the equilibrium surface. At cusp, $V''' = 0$, i.e.

$$u = u_1 = u_0 \left(\frac{m+1}{m} \right)^{1/m} \tag{9}$$

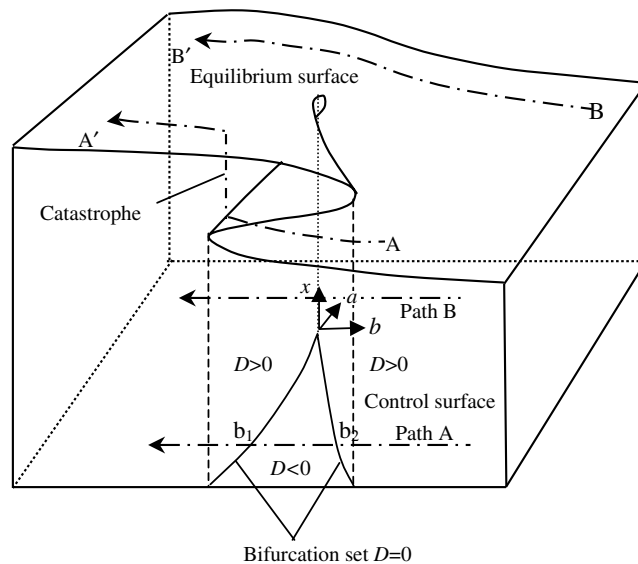


Fig. 3. Cusp catastrophe model.

Eq. (9) shows that the displacement value at cusp is exactly the displacement value at the turning point of the constitutive curve of the coal pillar.

Making Taylor series expansion with respect to u_1 for Eq. (8), discarding all the terms but the first three because the third order item is the minimum one away from zero, and substituting Eq. (9) into Eq. (8), one has

$$\begin{aligned} & \frac{1}{6}k_0m(m+1)^2 \exp\left(-\frac{m+1}{m}\right)u_1 \left\{ \left(\frac{u-u_1}{u_1}\right)^3 + \frac{6}{(m+1)^2} \left[\frac{24E_e I/l^3}{k_0m \exp\left(-\frac{m+1}{m}\right)} - 1 \right] \left(\frac{u-u_1}{u_1}\right) \right. \\ & \left. + \frac{6}{m(m+1)^2} \left[1 + \frac{24E_e I/l^3}{k_0 \exp\left(-\frac{m+1}{m}\right)} - \frac{ql}{k_0u_1} \exp\left(\frac{m+1}{m}\right) \right] \right\} = 0 \end{aligned} \quad (10)$$

In order to transform Eq. (10) into a standard form of cusp catastrophe, let

$$x = \frac{u-u_1}{u_1} \quad (11)$$

$$a = \frac{6}{(m+1)^2}(k-1) \quad (12)$$

$$b = \frac{6}{m(m+1)^2}(1+mk-\xi) \quad (13)$$

$$k = \frac{24E_e I/l^3}{k_0m \exp\left(-\frac{m+1}{m}\right)} = \frac{k_2}{k_1} \quad (14)$$

$$\xi = \frac{ql}{k_0u_1} \exp\left(\frac{m+1}{m}\right) \quad (15)$$

$$k_2 = \frac{24E_e I}{l^3} \quad (16)$$

$$k_1 = k_0m \exp\left(-\frac{m+1}{m}\right) = \frac{EA}{h}m \exp\left(-\frac{m+1}{m}\right) \quad (17)$$

where k is the ratio of the flexural stiffness k_2 of the beam to the absolute value k_1 of the stiffness at the turning point of the constitutive curve of the coal pillar (for simplicity, it is called hereafter the stiffness ratio); ξ is relative to the gravitational load intensity, geometric size of the system, and mechanical parameters of the coal pillar (referred to as the geometric-mechanical parameter).

Substituting Eqs. (11)–(15) into Eq. (10) leads to

$$x^3 + ax + b = 0 \quad (18)$$

Eq. (18) is the standard cusp catastrophe model of the equilibrium surface, with a and b as its control parameters and x as its state variable.

The cusp catastrophe described by the equilibrium surface containing fold or pleat is illustrated in Fig. 3 where axes of the three-dimensional space are the control parameters a , b (horizontal) and response parameter x (vertical). As pointed out by Henley (1976), path B–B' and path A–A' denote a stable evolutionary process and an unstable evolutionary process, respectively. The bifurcation set (cusp) (Thom, 1972) can be expressed as

$$D = 4a^3 + 27b^2 = 0 \quad (19)$$

Substituting Eqs. (12) and (13) into Eq. (19) leads to

$$D = 4\beta^3(k-1)^3 + 27\frac{\beta^2}{m^2}(1+mk-\xi)^2 = 0 \quad (20)$$

where $\beta = 6/(m+1)^2$.

The bifurcation set (Fig. 3) defines the thresholds where sudden changes can take place. As long as the state of the system remains outside the bifurcation set ($D > 0$), the behavior varies smoothly and continuously as a function of the control parameters. Even on entering the bifurcation set ($D < 0$) no abrupt change is observed. When the control point passes all the way through the bifurcation set ($D = 0$), however, a catastrophe is inevitable. Thus, Eq. (20) or (19) is the sufficient and necessary mechanical criteria for the instability of the coal-pillar-and-beam system. In the following analysis, D is referred to as the catastrophic characteristic index.

Clearly, only when $k \leq 1$, the condition of Eq. (20) may be satisfied. Thus, the necessary condition of instability is

$$k = \frac{24E_e I / l^3}{k_0 m \exp\left(-\frac{m+1}{m}\right)} \leq 1 \quad (21)$$

Eq. (21) shows that the smaller the flexural stiffness of the beam is, the larger the post-peak stiffness (the absolute value of post-peak constitutive curve slope) of the coal pillar, and the more possible it is for the system to lead to catastrophe. It is known from Eq. (21) that k decreases with an increase of m for the fixed values of $24E_e I / k_0 l^3$, demonstrating that a more homogeneous coal pillar is more prone to bump.

2.3. Relation between the post-peak stiffness and dimension and water content for coal pillar

It is well known that the mechanical properties of rock or coal specimens are scale dependent. It is seen from Fig. 4 that, for the rock specimens with different ratios of length to diameter, their initial stiffness values of k_0 are unchanged, but the post-peak stiffness increases as the ratios of length to diameter increase. This demonstrates that a higher coal pillar with a smaller diameter will correspond to a larger post-peak stiffness value of the coal pillar and hence a smaller stiffness ratio of the system, which is more prone to bump.

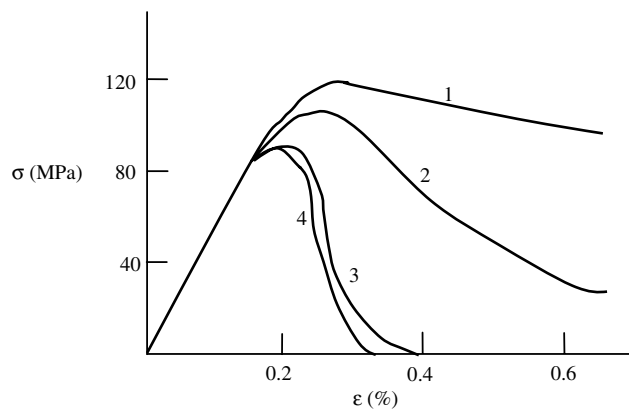


Fig. 4. Stress–strain curves of marble specimens with different ratios of length to diameter under axial compression condition (the ratios of length to diameter for specimens 1–4 are 0.5, 1, 2 and 3, respectively; modified from Hudson et al., 1972).

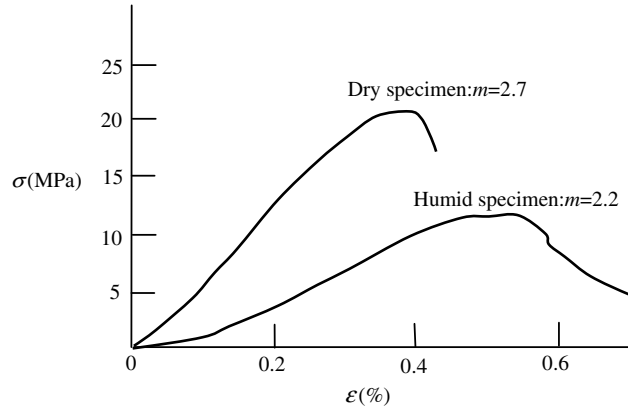


Fig. 5. Influences of water on the stress–strain curves of coal specimens (modified from Fei et al., 1995).

Fig. 5 shows that water can reduce the initial stiffness k_0 and the homogeneity index m . This will result in a larger stiffness ratio of the system and accordingly a more stable system, implying that an increase of water content in the coal pillar can reduce the possibility of a bump.

2.4. Instability mechanisms of system

Only when the stiffness ratio and homogeneity index as well as the geometric-mechanical parameter satisfy Eq. (20), a bump can occur. This condition may be met only after the deformation of a coal pillar enters into the strain-softening phase. If $k > 1$, after entering into the post-peak strain-softening phase, the deformation of the coal pillar can behave as progressive failures, not leading to bump. When $k \leq 1$ and $D \rightarrow 0$, i.e., the system is close to a critical state, whether or not a bump occurs depends on the external disturbance, such as vibrations caused by blasting. In the case that the instability of the system is triggered by such disturbance, the coal pillar can generate a sudden deformation and quickly release energy, i.e. occurrence of a bump. Thus, it can be concluded from the above discussion that the occurrence of a bump is not due to the inadequate strength of the system, but due to the smaller stiffness ratio of the system, and is triggered by the external disturbance. In other words, the bump is a physical unstable phenomenon. It is worth noting that as the excavation width increases, the flexural stiffness of the beam will decrease drastically and hence the condition $k \geq 1$ is readily met.

Eq. (18) ($b < 0$) and Eq. (19) can be used to determine the critical displacement value at the unstable points corresponding to coal bump as follows:

$$u_b = u_1 \left[1 - \frac{\sqrt{2}}{m+1} (1-k)^{1/2} \right] (k \geq 1) \quad (22)$$

2.5. Case study

According to field investigations and laboratory experiments for the excavation zone 51 in the Mentougou coal mine, PR China (Qin et al., 1993), the average thickness h_b and the Young's modulus E_c of the quartz sandstone above the coal seam is 10 m and 59.5 GPa, respectively. The height h and the initial stiffness k_0 of the coal pillar are 3.5 m and 71.43 GN/m, respectively. The parameters ε_0 and m of the coal pillar can be determined by fitting the experimental data with Eq. (2) by the least square fitting method (Fig. 6).

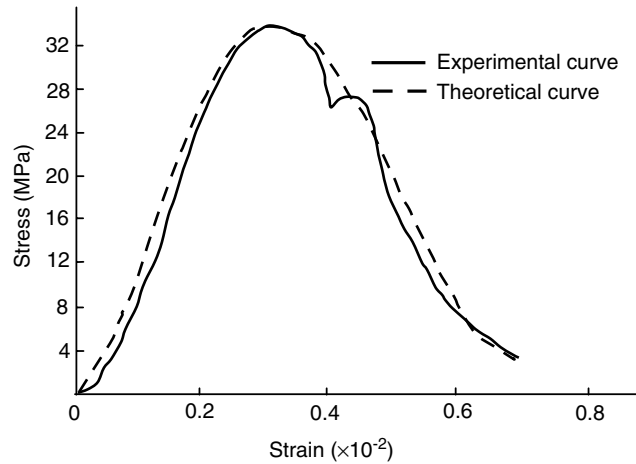


Fig. 6. Experimental and theoretical curves of coal specimen under uniaxial compression.

We obtain $\varepsilon_0 = 0.0028$ (which leads to $u_0 = h\varepsilon_0 = 0.0098m$) and $m = 2.24$. The distance between the top of the quartz sandstone and ground surface is about 390 m and hence the gravitational load intensity q is 0.01 GPa (the average unit weight of the beam and the upper strata is assumed to be 25 kN/m^3).

Substituting the known parameters into Eq. (20), the critical excavation width l of the coal chamber is calculated as 22.89 m and the stiffness ratio is 0.263 (<1). This width is close to the actual excavation width of 24.9 m when a coal bump occurred.

3. Nonlinear dynamical model of evolutionary process of system

In the above analysis, we considered the quasi-static motion process of the coal-pillar-and-beam system, but not the dynamical process of instability. To study the physical prediction of coal bump, a nonlinear dynamical model is needed.

3.1. Nonlinear dynamical model

If the viscosity or creeping (i.e. time-dependent) property of the coal pillar is considered (Fig. 7), then its uniaxial compression stress can be expressed as

$$\sigma = \sigma_e + \sigma_\eta = E\varepsilon \exp \left[-\left(\frac{\varepsilon}{\varepsilon_0}\right)^m \right] + \eta \frac{d\varepsilon}{dt} \tag{23}$$

where η is the viscosity coefficient. After transforming Eq. (23) into the form of the load P and deformation u , substituting it into the Eq. (8), making Taylor series expansion with respect to u_1 and using Eqs. (11)–(15), one obtains

$$\begin{aligned} \frac{\eta A}{h} \frac{du}{dt} &= - \left\{ k_0 u \exp \left[-\left(\frac{u}{u_0}\right)^m \right] + \frac{24E_e I}{l^3} u - ql \right\} \\ &= -\frac{1}{6} k_0 m(m+1)^2 \exp \left(-\frac{m+1}{m} \right) u_1 (x^3 + ax + b) \end{aligned} \tag{24}$$

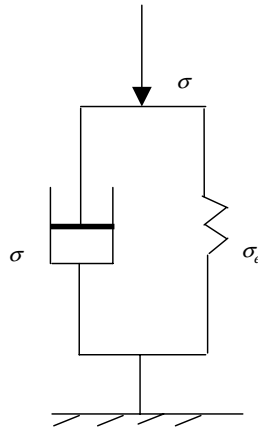


Fig. 7. A stress model considering the viscosity or creeping property of coal pillar, similar to Kelvin or Voigt model.

Eq. (24) can be further simplified as

$$\frac{dx}{dt} = -\frac{1}{6} \frac{E \exp\left(-\frac{m+1}{m}\right) m(m+1)^2}{\eta} (x^3 + ax + b) \quad (25)$$

Eq. (25) is a nonlinear dynamical or physical forecasting model with a well-defined physical meaning for each parameter. As long as we know the parameters of the model by means of the laboratory test and field investigation, the physical prediction of the deformation rule of the system can be made. It is known from the above-mentioned analysis that the parameters a and b denote the possibility of instability and the creeping phase of a coal pillar, respectively. Obviously, the dimensionless displacement rate grows as the parameter b ($b < 0$) decreases when $a < 0$.

The character of the equilibrium state of Eq. (25) will be now discussed. It is known by letting $dx/dt = 0$ that Eq. (25) also is a cusp catastrophe and its instability condition is the same as Eq. (18).

Eq. (25) demonstrates that the dimensionless displacement x is wholly dominated by the mechanical and geometric parameter of the system itself. Thus, it is deduced that the variations of the mechanical parameters can be reflected in the observed displacement-time series of a roof or a coal pillar when the geometric parameters are fixed, which demonstrates that we can estimate the mechanical parameters from the observation series using an algorithm of inversion.

3.2. Algorithm of inversion on the nonlinear dynamical model

The only information available at present is the observation data and description of deformation and failure phenomena for the complex evolutionary process of rockbursts and bumps. That is to say, we know a series of specific solutions of the dynamical model. If we regard such solutions as a series of discrete values of the dynamical model, the quasi-ideal nonlinear dynamical model for the evolution of the rockburst and bump can, thus, be obtained through an algorithm of inversion. The following gives the analytical procedures and steps.

(1) Substituting Eq. (11) into Eq. (25) in order to transforming $x - t$ series into $u - t$ series, one has

$$\frac{du}{dt} = c_1 u^3 + c_2 u^2 + c_3 u + c_4 \quad (26)$$

where

$$c = -E \exp\left(-\frac{m+1}{m}\right) m(m+1)^2 / 6\eta \quad (27)$$

$$c_1 = c/u_1^2 \quad (28)$$

$$c_2 = -3c/u_1 \quad (29)$$

$$c_3 = (3+a)c \quad (30)$$

$$c_4 = [b - (a+1)]cu_1 \quad (31)$$

(2) The parameters c_1 , c_2 , c_3 and c_4 can be solved by best fitting the original observation data with Eq. (26) by a fitting algorithm. It should be noted (Bakus and Gilbert, 1970) that, in most cases, the solutions of Eq. (26) usually are unstable when the least squares method is adopted. Therefore, it is suggested that an improved iterative algorithm of inversion presented by Qin et al. (2002) can be applied to the solution of Eq. (26). The predicted values can be calculated using the Runge–Kutta integration method for Eq. (26).

3.3. Case study

The average coal seam thickness at the excavation zone 741003 in the Qianjuntai pit of the Muchengjian coal mine, PR China, is 2.6 m (Tan and Wang, 1992). The roof rocks are mainly composed of hard layered sandstone with an uniaxial compression strength of more than 100 MPa and an average thickness of 5 m. An automatic monitoring system is used for monitoring the roof settlement and AE activity. A coal bump occurred at about 8 o'clock on 18 June 1990.

Based on the observed roof settlement data in Fig. 8, the nonlinear dynamical model obtained using the above-mentioned algorithm of inversion is as follows:

$$\frac{dx}{dt} = -0.08513(x^3 - 3.028x - 1.8367) \quad (32)$$

Fig. 8 shows that the predicted values are in relatively good agreement with the observed values. By choosing the data between the beginning of observation and a certain time, we can get a series of values for a , b and D . It is observed from Fig. 8 that the catastrophic characteristic index D behaves as a steady variation at the beginning, then, it begins to have a rapid increase and reaches an extremely high peak value (about 5000 times larger than the steady value), and eventually it quickly falls to approximately zero prior to

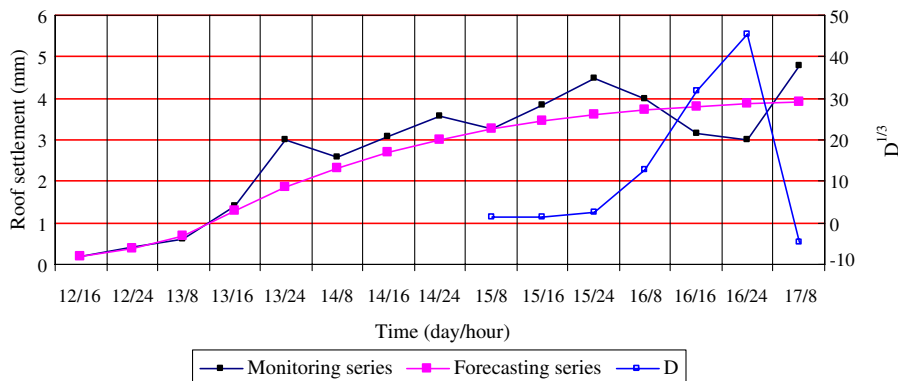


Fig. 8. Curves of the monitoring values, forecasting ones and the catastrophic characteristic indexes D versus time at the working surface 741003 in the Qianjuntai pit of the Muchengjian coal mine, Beijing mining bureau, PR China, from 12 June to 17 June 1990.

oncoming coal bump as expected, showing that the system has approached to or reached a critical state and that a coal bump will occur under adequate external disturbances. A strong explosion vibration in the morning of 18 June 1990 may trigger this bump. Also, this phenomenon is similar to the mutative character of D in the study of landslides using the catastrophe theory presented by Qin et al. (1993). Thus, the index D can be regarded as an important index indicating the precursory abnormality of coal bump.

4. Nonlinear dynamical model of AE and AE characteristics in the evolutionary process of system

4.1. Model

AE is transient elastic waves generated by the rapid releases of elastic energy due to local micro-rupturing as the results of local damage. Qin et al. (1993) and Tang (1993) studied the relationship between the damage parameter $D(\varepsilon)$ and the accumulative AE counts N of rock specimens under uniaxial stress state as the following

$$N = N_m D(\varepsilon) = N_m \left\{ 1 - \exp \left[- \left(\frac{\varepsilon}{\varepsilon_0} \right)^m \right] \right\} \quad (33)$$

where N_m is the accumulative AE counts when the rock specimen is completely damaged. In order to obtain the function of AE rate (AER), Eq. (33) can be differentiated with respect to time t , which gives,

$$\frac{dN}{dt} = N_m \frac{m}{\varepsilon_0} \left(\frac{\varepsilon}{\varepsilon_0} \right)^{m-1} \exp \left[- \left(\frac{\varepsilon}{\varepsilon_0} \right)^m \right] \frac{d\varepsilon}{dt} \quad (34)$$

Using Eqs. (9) and (11), Eq. (34) can be rewritten in the form of the dimensionless displacement x as

$$\frac{dN}{dt} = N_m (m+1) (x+1)^{m-1} \exp \left[- \left(\frac{m+1}{m} \right) (x+1)^m \right] \frac{dx}{dt} \quad (35)$$

In the above-mentioned analysis, we practically assumed that the statistical distribution of strength of local elements along a cross section of the coal pillar follows the Weibull's distribution. However, the strength distribution of these elements along the height of the coal pillar is probably random. Thus, Eq. (35) is multiplied with a factor, RND , which has a random value between 0 and 1 generated by a computer, that is

$$\frac{dN}{dt} = RND(x) N_m (m+1) (x+1)^{m-1} \exp \left[- \left(\frac{m+1}{m} \right) (x+1)^m \right] \frac{dx}{dt} \quad (36)$$

It is found by comparisons with and without RND that RND only has an impact on the AER magnitude but does not affect the AER patterns and rules.

For a strong roof and floor, as pointed out by Kaiser and Tang (1998), AE or seismicity is almost exclusively confined to the pillar. Thus, AE mainly comes from the progressive failures of the coal pillar. Substituting Eq. (25) into Eq. (36) leads to

$$\frac{dN}{dt} = - \frac{1}{6} \frac{E}{\eta} RND(x) N_m \alpha(m) (x+1)^{m+1} \exp \left[- \left(\frac{m+1}{m} \right) (x+1)^m \right] (x^3 + ax + b) \quad (37)$$

where

$$\alpha(m) = \frac{m(m+1)^3}{\exp \left(\frac{m+1}{m} \right)} \quad (38)$$

Eq. (37) is the AER expression in the evolutionary process of the coal-pillar-and-roof system. This expression is related to the elastic modulus, the viscosity coefficient and the homogeneity index (or brittleness index) of the coal pillar as well as the control parameters of the system. It is seen from Eq. (37) that E and η only affect the AER magnitude but do not change the evolutionary modes of AER.

4.2. AE patterns and characteristics in the deformation process of system

Eq. (37) can be used for modeling the AER features in the evolutionary process of the coal-pillar-and-roof system. For simplicity, let $E/\eta = 0.01$, $N_m = 10000$, $k_0 = 1000$, $u_0 = 0.2$ and the parameters used satisfy the necessary-sufficient condition of instability, $D = 0$, for analyzing the influences of the stiffness ratio k and the homogeneity index m on AER. The simulations are conducted in a displacement control mode.

Xie and Pariseau (1993) found that, just before the rockbursts, the micro-seismic frequency increased 10–100 times more than the normal noise frequency, then quickly dropped. This dropping phenomenon is called as the seismicity anomaly. It has been observed that seismicity anomaly appeared usually prior to rockbursting, and that some of rockbursts occurred in an active period of seismicity but some of them did in a relative quiescence period. These observations are consistent with the AER variational rules as illustrated in Figs. 9, 11, 12 modeled with different values of m , i.e., the rockbursts or bumps occur in the dropping or relative quiescence period of AE activities after rising.

Figs. 9–12 show that as m increases, i.e., the homogeneity or brittleness of the coal pillar increases, the concentration phase of AE activities will transfer from the phase far from the pre-peak load through the phase near the peak load, to the post-peak load phase. Also, it is observed that the AER magnitude rises as m increases, demonstrating that a more homogeneous or brittle coal pillar will release greater energy and lead to a more violent coal bump.

Figs. 10–12 show three main patterns of AE sequences: (1) “swarm” pattern related to heterogeneous material, as illustrated in Fig. 10 for $m = 5$; (2) “foreshock–main shock–aftershock” pattern related to moderately homogeneous material, as illustrated in Fig. 11 for $m = 20$; and “main shock” pattern related to homogeneous material, as illustrated in Fig. 12 for $m = 80$. These observations are consistent with find-

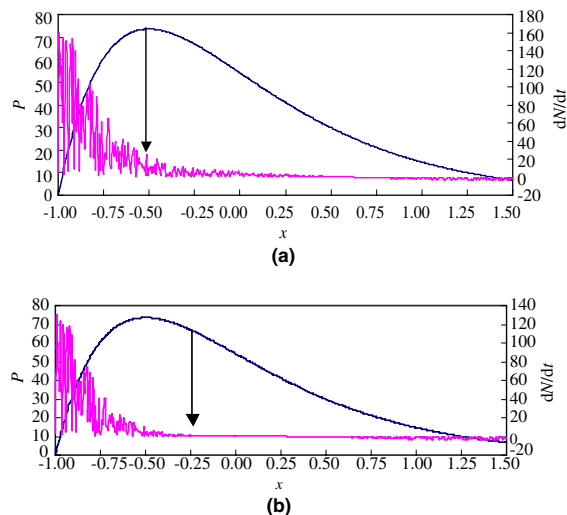


Fig. 9. Curves of load P and AER versus dimensionless displacement x when $m = 1$ and $D = 0$ (the arrow denotes the occurrence point of coal bump). (a) $k = 0.5$ and (b) $k = 0.9$.

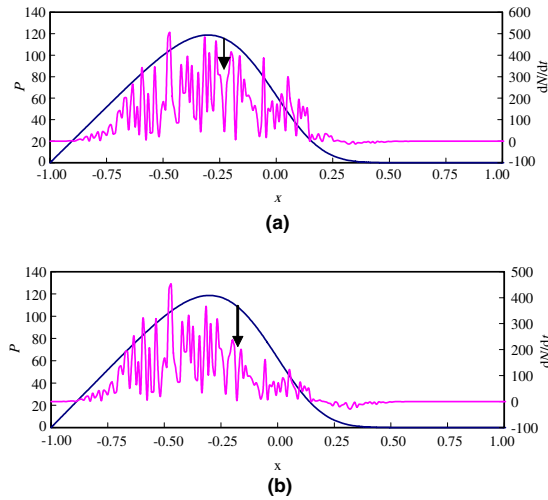


Fig. 10. Curves of load P and AER versus dimensionless displacement x when $m = 5$ and $D = 0$ (the arrow denotes the occurrence point of coal bump). (a) $k = 0.1$ (b) $k = 0.5$.

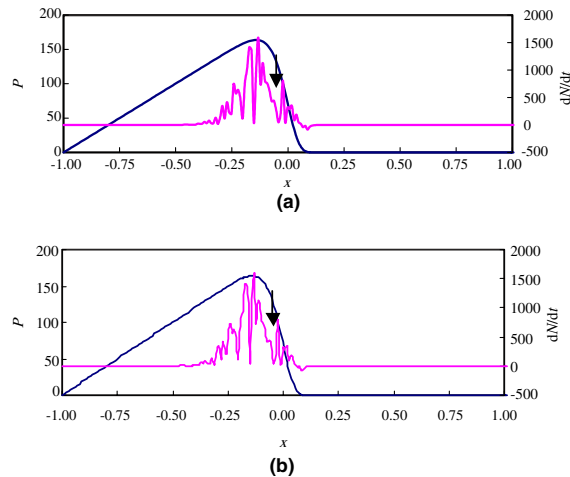


Fig. 11. Curves of load P and AER versus dimensionless displacement x when $m = 20$ and $D = 0$ (the arrow denotes the occurrence point of coal bump) (a) $k = 0.1$ and (b) $k = 0.5$.

ings presented by Mogi (1985) based on his experimental work. He showed that differences in structural homogeneity result in different AE patterns.

For the same values of m , the displacement values corresponding to instability points increase and the AER magnitudes decrease as k increases. When $m = 1$ (Fig. 9b), since AE activities prior to instability drop and a quiescence period appears, it is difficult to make a successful prediction of the bump because the feint from anomaly to transforming into quiescence in AE could be confusing. When $m = 5$ (Fig. 10), AE activities behave as a “swarm” pattern, implying that it also is difficult to predict the bump successfully. When

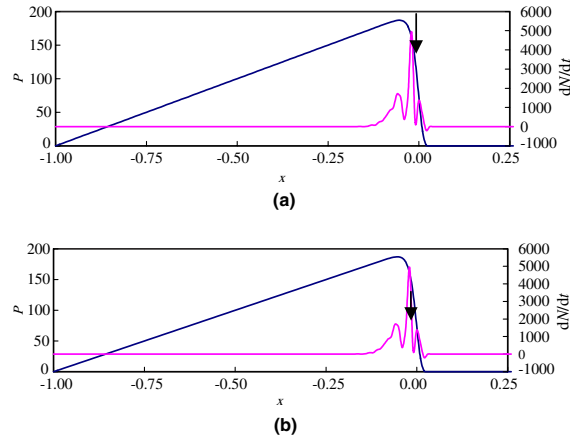


Fig. 12. Curves of load P and AER versus dimensionless displacement x when $m = 80$ and $D = 0$ (the arrow denotes the occurrence point of coal bump). (a) $k = 0.1$ and (b) $k = 0.5$.

$m = 20$ (Fig. 11), we can likely make a successful prediction of the bump due to the emergence of evident precursory anomalies. When $m = 80$ (Fig. 12), a prediction of bump is difficult to make due to un conspicuous and very short-period precursory anomalies close to instability. Thus it can be concluded that the predictability of instability for the coal-pillar-and-roof system relies mainly on the homogeneity or brittleness index m of the coal pillar. The predictions of bump are difficult for too great or too small values of m . Here, we emphasize that a better forecasting approach is to conduct a physical prediction by using Eq. (37) and combining the experiment tests for determining the parameters m, k , etc., with monitoring of the roof settlement and AE activities in the coal pillar.

In order to compare the AER mutative features between the cases when a bump ($D = 0$) occurs or not ($D \neq 0$), we will analyze further by taking Fig. 13 as an example. It is found from Fig. 13 that when there is a bump, the AE active period appears prior to the peak load and the AE activities prior to instability drop obviously. It is also found that when there is not a bump, the AE activities with higher AER values are

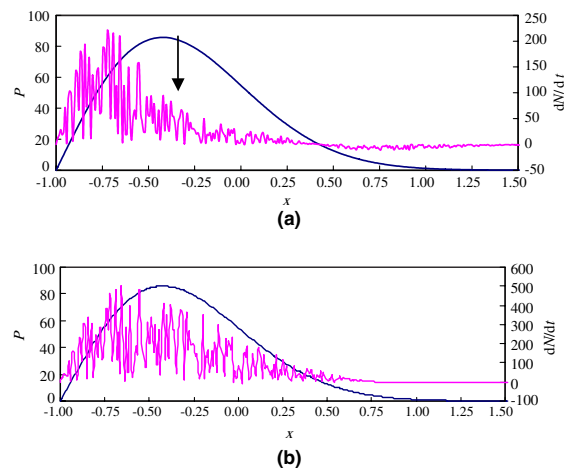


Fig. 13. Curves of load P and AER versus dimensionless displacement x when $m = 2$ and $k = 0.5$. (a) $D = 0$ (occurrence of coal bump) and (b) $D \neq 0$ (nonoccurrence of coal bump).

active at all times before and after the peak load, and are with a relatively long-period duration. This shows that the coal pillar's failures are in a progressive manner not leading to a bump. During the monitoring of a real coal mine, if a sudden dropping or quiescence period is observed after the AE activities are active, we should pay more attentions to this phenomenon and make a synthetical judgment for forecasting a bump according to in situ investigations and the other precursory phenomena.

The above-mentioned analysis shows that the AE activities rely on not only the homogeneity index m and the stiffness ratio k , but also the control parameters a and b as well as the catastrophic characteristic index D . In other words, the AE feature of the system is related to its evolutionary path ($D = 0$ or $D \neq 0$). Also, the AE images are distinctly different for an unstable and stable systems.

5. Conclusions

This paper presents a theoretical framework that explicitly links observation data of roof settlement or coal-pillar deformation and AE with a nonlinear dynamical model, so that we can improve our way to predict the coal bump. The models and approaches put forward in this paper may open a new way to study the complexity of the bump mechanisms.

The following conclusions are obtained from the above analysis:

1. Taking the stiff roof as an elastic beam and the coal pillar as a strain-softening medium, whose constitutive model is described by the Weibull's theory of the strength of materials, we studied the instability leading to coal bump for the coal-pillar-and-roof system using the catastrophe theory. It is found that the instability of the system depends mainly on the ratio of the flexural stiffness of the beam to the absolute value of the stiffness at the turning point of the constitutive curve of the coal pillar and the homogeneity index (also called the brittleness index) of the coal pillar. The sufficient-necessary conditions leading to coal bump are also presented and are proved to be effective by a case study of the excavation zone 51 in the Mentougou coal mine, PR China.
2. By considering the viscosity property or the time-dependent behavior of the coal pillar medium, a nonlinear dynamical model (or called a physical prediction model) is presented. This model can be used to study the physical prediction of the deformation rule for the coal-pillar-and-roof system according to the mechanical parameters determined from the laboratory experiments and the geometric parameters by the field investigations.
3. The nonlinear dynamical analysis on the observed roof settlement data at the excavation zone 741003 in the Qianjuntai pit of the Muchengjian coal mine, PR China, shows that the catastrophic characteristic index D has a steady variation first when the system is far from the instability, and then shows a quick rise till reaching an extremely high peak value, and finally drops drastically to some value less than zero prior to instability. We can judge the occurrence of coal bump from this specific feature and regard the index D as a parameter reflecting the precursory abnormality of a bump.
4. A dynamical model of AE is established from the viewpoint of damage mechanics of a coal pillar. It is found by numerical simulations that the homogeneity index m of the coal pillar and the evolutionary path ($D = 0$ for instability or $D \neq 0$ for stability) of the system have a great impact on the AE rules and patterns. The predictability of bumps depends greatly on the values of m , i.e., the prediction of a bump is difficult to make for very homogeneous (large value of m) or very heterogeneous (small value of m) coal pillars.

Acknowledgement

The work was funded by China national 973 programme (No. 2002CB412702).

References

- Bakus, G., Gilbert, F., 1970. Uniqueness in the inversion of inaccurate gross earth data. *Philos. Trans. R. Soc. London, Ser. A266* (1173), 123–192.
- Chen, Z.H., Tang, C.A., Huang, R.Q., 1997. A double rock sample model for rockbursts. *Int. J. Rock Mech. Min. Sci.* 34 (6), 991–1000.
- Cook, N.G.W., 1965. A note on rockburst considered as a problem of stability. *J. South Afr. Int. Min. Metall.* 65, 437–446.
- Fei, H.L., Tang, C.A., Xu, X.H., 1995. Study of rock instability under uniaxial loading by catastrophe theory. *Chin. J. Nonferrous Met. Soc.* 5 (4), 31–34.
- Henley, S., 1976. Catastrophe theory models in geology. *Math. Geol.* 8 (6), 649–655.
- Hudson, J.A., Fairhurst, C., 1969. Tensile strength, Weibull's theory and a general statistical approach to rock failure. In: Teeni, M., (Ed.). *The Proceedings of the Southampton 1969 Civil Engineering Materials Conference (Part 2)*, pp. 901–904.
- Hudson, J.A., Crouch, S.L., Fairhurst, C., 1972. Soft, stiff and servo-controlled testing machine: a review with reference to rock failure. *Eng. Geol.* 6, 155–189.
- Kaiser, P.K., 1995. Observational modeling approach for design of underground excavations. In: *Proceedings of International Workshop on Observational Method of Constructions of Large Underground Caverns in Difficult Ground Conditions*, Tokyo. pp. 1–7.
- Kaiser, P.K., Tang, C.A., 1998. Numerical simulation of damage accumulation and seismic energy release during brittle rock failure—Part II: Rib pillar collapse. *Int. J. Rock Mech. Min. Sci.* 35 (2), 123–134.
- Kaiser, P.K., Tannant, D.D., McCreath, D.R., 1995. Support of tunnels in burst prone ground. In: *Proceedings of 8th International Congress on Rock Mechanisms*, Tokyo, vol. 2, pp. 471–477.
- Krajcinovic, D., Silva, M.D., 1982. Statistical aspects of the continuous damage theory. *Int. J. Solids Struct.* 18, 551–562.
- Liu, H.W., 1991. *Material Mechanics* (in Chinese). Higher Education Press, Beijing.
- Mogi, K., 1985. *Earthquake Prediction*. Academic Press, Harcourt Brace Jovanovich Publishers, Tokyo.
- Pan, Y.S., Zhang, M.T., 1992. Analysis on the physical process of rockbursts by catastrophe theory (in Chinese). *J. Fuxin Mining Inst.* 11 (1), 12–18.
- Qin, S.Q., Zhang, Z.Y., Wang, S.T., 1993. *An Introduction to Nonlinear Engineering Geology*. Southwest University Press of Transportation, Chengdu, PR China.
- Qin, S.Q., Wang, S., Long, H., Liu, J., 1999. A new approach to estimating geo-stresses from laboratory Kaiser effect measurements. *Int. J. Rock Mech. Min. Sci.* 36, 1073–1077.
- Qin, S.Q., Jiao, J.J., Wang, S.J., 2001. A nonlinear catastrophe model of instability of planar-slip slope and chaotic dynamical mechanisms of its evolutionary process. *Int. J. Solids Struct.* 38, 8093–8109.
- Qin, S.Q., Jiao, J.J., Wang, S.J., 2002. A nonlinear dynamical model of landslide evolution. *Geomorphology* 43, 77–85.
- Salamon, M.D.G., 1993. Keynote address: some applications of geomechanical modeling and related research. In: Young, A.A. (Ed.), *Rockburst and Seismicity in Mines, Proceedings of the 3rd International Symposium*. Balkema, Rotterdam, pp. 279–309.
- Tan, Y.L., Wang, X.S., 1992. A preliminary study of acoustic emission of rock during the roof weighting process in a coal mine. *Chinese J. Rock Mech. Eng.* 11 (3), 275–283.
- Tang, C.A., 1993. *Catastrophe in Rock Unstable Failure* (in Chinese). China Coal Industry Publishing House, Beijing.
- Tang, C.A., Hudson, J.A., Xu, X.H., 1993. *Rock Failure Instability and Related Aspects of Earthquake Mechanisms*. China Coal Industry Press, Beijing.
- Thom, R., 1972. *Stabilité Structurale et Morphogénèse*. Benjamin, New York.
- Wang, J.A., Park, H.D., 2001. Comprehensive prediction of rockburst based on analysis of strain energy in rocks. *Tunnelling and Underground Space Technology* 16, 49–57.
- Xie, H., Pariseau, W.G., 1993. Fractal character and mechanism of rock bursts. *Int. J. Rock Mech. Min. Sci. Geomech. Abstr.* 30, 343–350.
- Xu, Z.H., Xu, X.H., Tang, C.A., 1995. Analysis of a cusp catastrophe bump of coal pillar under hard rocks. *J. China Coal Soc.* 20 (5), 191–485.